Electronic Supplementary Material (ESI) for Physical Chemistry Chemical Physics.

Manipulating the Charge Transport via Incorporating Cobalt Bridge into Single-Molecule Junction

Table of Contents

1. General Information

All reactions were carried out under nitrogen atmosphere and anhydrous conditions unless otherwise indicated. All manipulations of air-sensitive or moisture-sensitive compounds were performed in a glovebox under an atmosphere of nitrogen. Unless otherwise noted, all catalytic reactions were run in dried glassware. Other commercial reagents were purchased from Bidepharm, jiudingchem, Adamas-beta China and were used as received. Reactions were monitored by thin-layer chromatography (TLC) carried out on 0.20 mm silica gel plates using UV light as the visualizing agent.

2. Experimental Section

2.1 Synthesis

p-p, **m-m**, **p-m** were prepared via Sonogashira coupling reported by other literatures.[1]
p=p and **m=m** were prepared via wittig reaction reported by other literatures.[2]
p-Co-p, **m-Co-m** and **p-Co-m** were prepared using $Co_2(CO)_8$ reported by other literatures.[3]

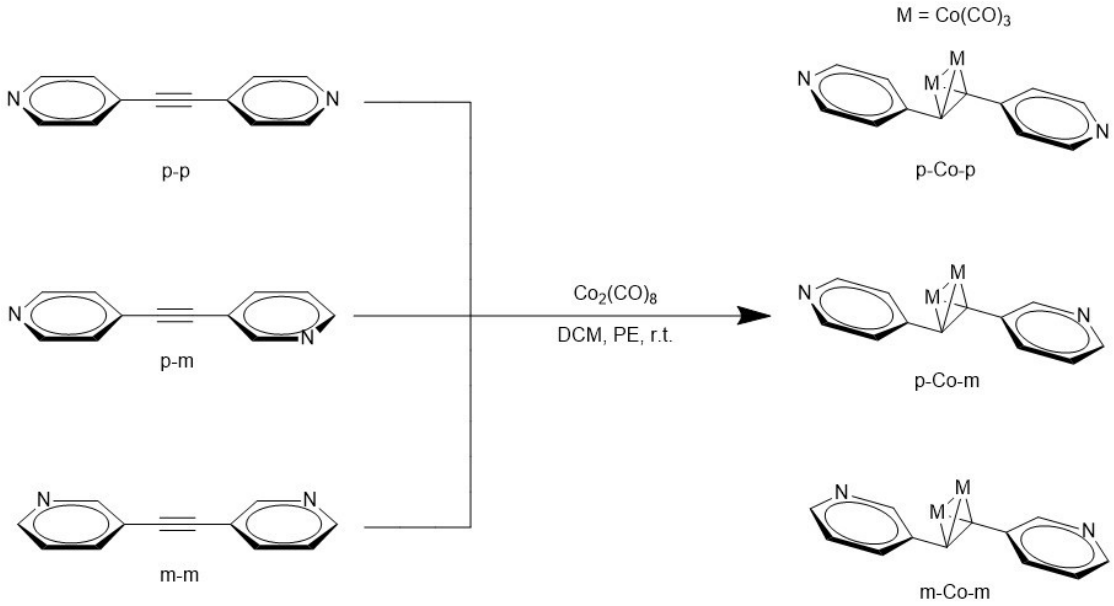

Scheme S1 The synthetic route of the target molecules **p-Co-p**, **m-Co-m** and **p-Co-m**

General procedure A for Co-bridged organometallic molecular wires:

A Schlenk flask was charged with alkynes, 2.5 mL of CH_2Cl_2, and 5 mL of petroleum ether. While stirring, a solution of 0.170 g (0.5 mmol) of $Co_2(CO)_8$ in 5 mL of petroleum ether was slowly added. The mixture was stirred at room temperature for 2-3 h until no CO evolution was observed. Solvent was removed under reduced pressure, and the residue was subjected to filtration chromatography using acetone as eluent. Removal of the solvent gave a crystalline dark red solid.

p-Co-p

Crystalline dark red solid. Yield: 73%. TOF-MS: $[M+H]^+$ Calcd for $C_{18}H_9N_2O_6Co_2$: 467.1711; found: 466.9125. IR(KBr): $\nu_{C=O}$ 2090.0, 2024.6 cm^{-1}.

m-Co-m

Crystalline dark red solid. Yield: 65%. TOF-MS: $[M+H]^+$ Calcd for $C_{18}H_9N_2O_6Co_2$: 467.0786; found: 466.9125. IR (KBr): $\nu_{C=O}$ 2090.5, 2010.1 cm^{-1}.

p-Co-m

Crystalline dark red solid. Yield: 63%. TOF-MS: $[M+Na]^+$ Calcd for $C_{18}H_8N_2O_6Co_2Na$: 487.9789; found: 488.8944. IR (KBr): $\nu_{C=O}$ 2090.6, 2021.0 cm^{-1}.

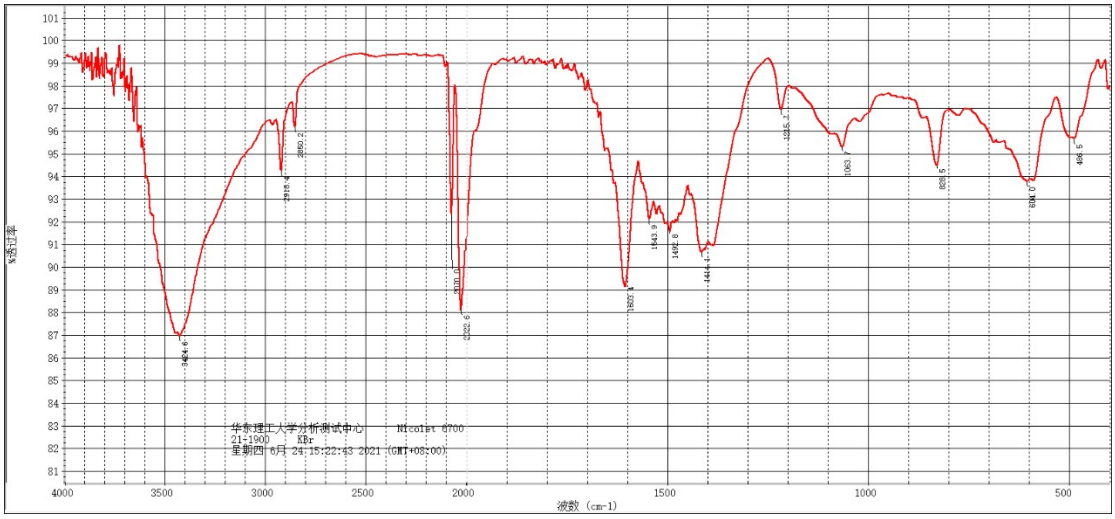

Figure S1. FTIR-spectrum of **p-Co-p**

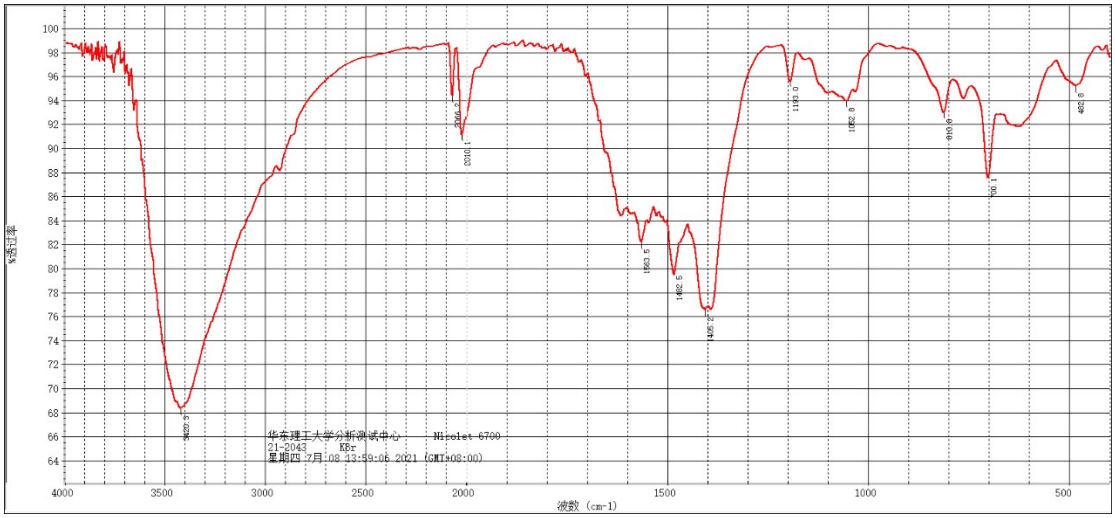

Figure S2. FTIR-spectrum of **m-Co-m**

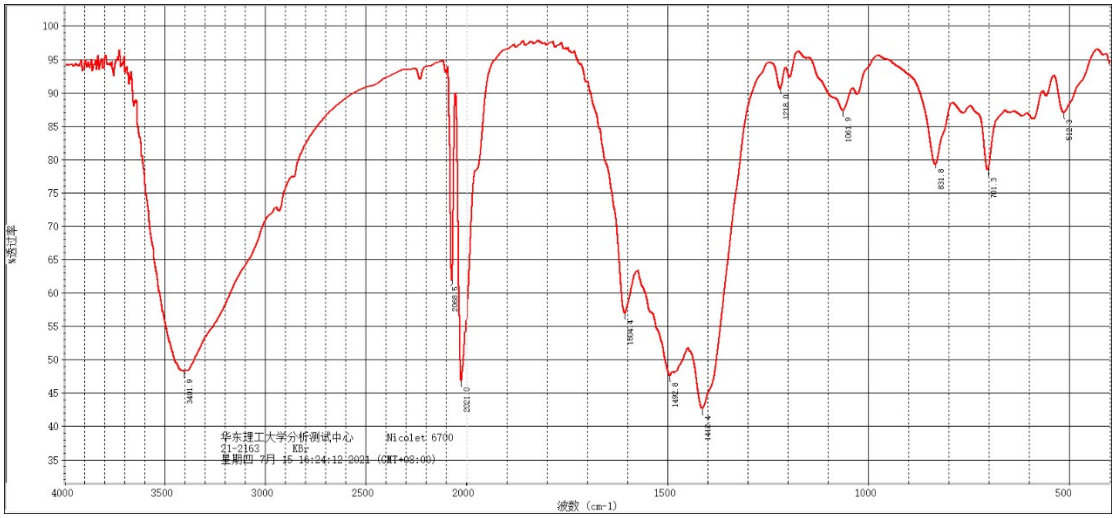

Figure S3. FTIR-spectrum of **p-Co-m**

2.2 Conductance measurements

The conductance was measured by using the Xtech STM break-junction technique under ambient conditions (room temperature 25°C), and the data is analyzed by XMe open-source code. More information is reported on previous papers [4-8]. The STMBJ measurements were performed in TCB (1,2,4-trichlorobenzene, CNW Technologies) with a concentration of 0.1 mM.

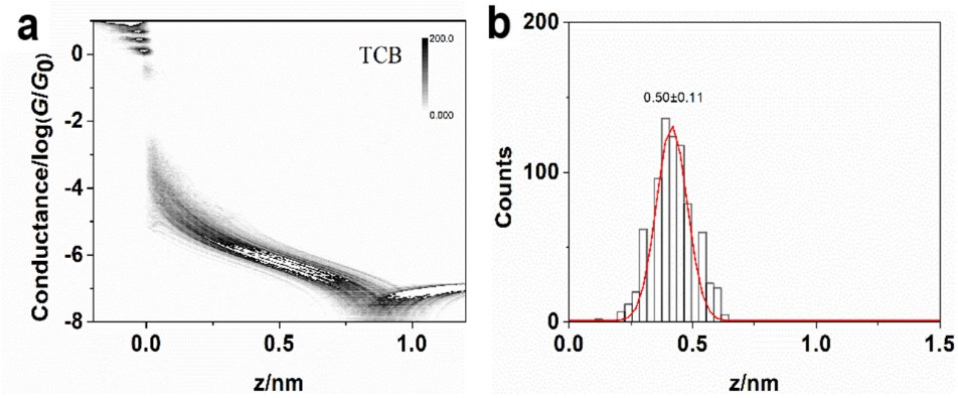

Figure S4. (a) Two-dimensional conductance histogram of blank solvent. (b) Relative displacement distribution. The conductance ranges to determine the relative displacement distribution are from $10^{-0.3}$ $10^{-6.0}$ G_0. No obvious conductance peak signal was found in the blank solvent measurement. The stretching distance is Δz=0.50±0.11 nm (the error is the standard deviation), corresponding to the gold snap-back distance.

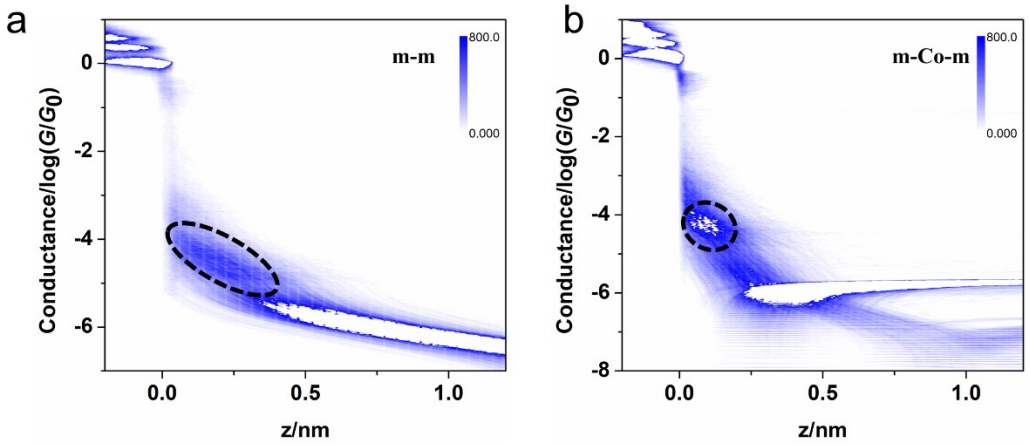

Figure S5. (a) 2D conductance histograms of **m-m**. (b) 2D conductance histograms of **m-Co-m**.

According to the 2D conductance histograms, the introduction of cobalt bridges largely shortened the molecular length.

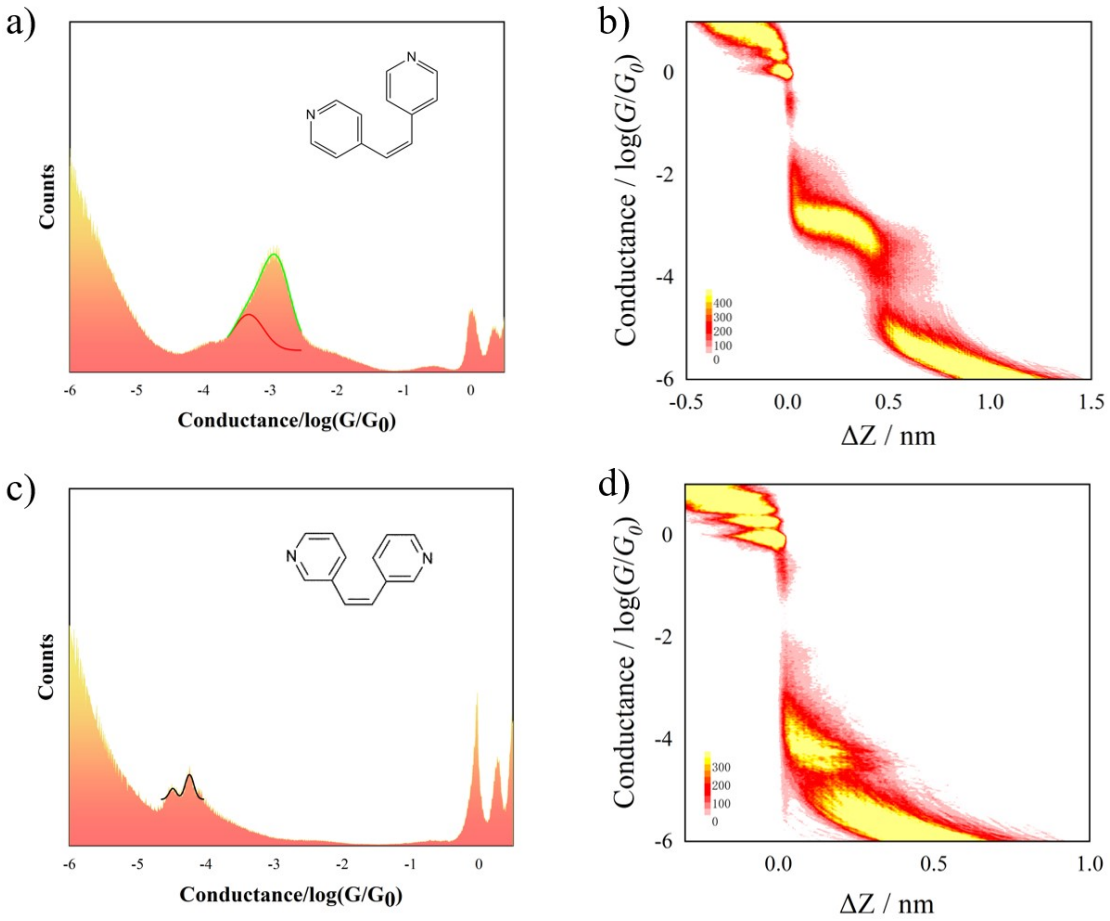

Figure S6. (a) 1D conductance histograms of **p=p**. (b) 2D conductance histograms of **p=p**. (c) 1D conductance histograms of **m=m**. (d) 2D conductance histograms of **m=m**.

The *cis*-compounds are unstable and convert to *trans*-compounds under the electric field. We can find an extra conductance peak in (a) and (c) which belongs to the corresponding trans-compounds.

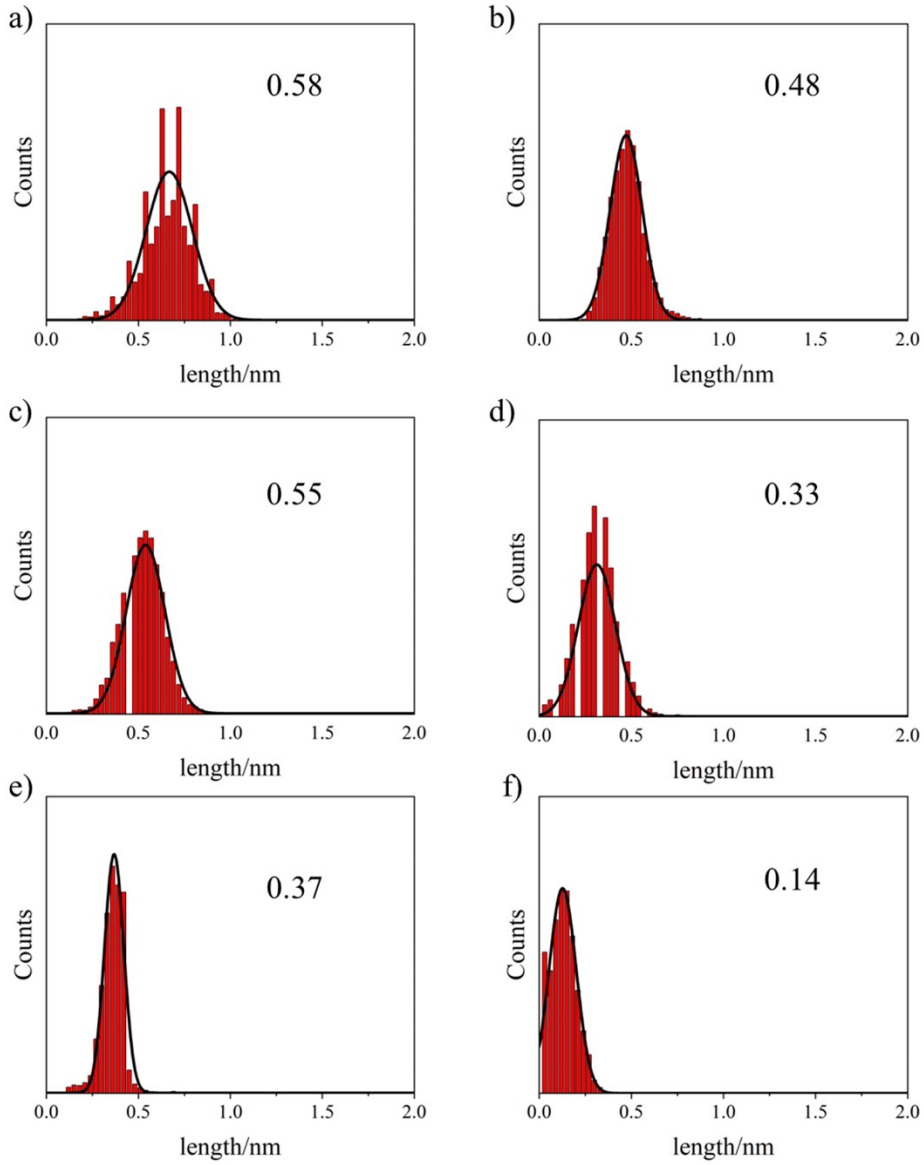

Figure S7. Displacement distribution histograms of single molecular junctions with molecules. (a) **p-p**, (b)**p-Co-p**, (c) **p-m**, (d) **p-Co-m**, (e)**m-m**, (f)**m-Co-m.** According to the displacement distribution histograms, we can observe the molecular lengths decline clearly.

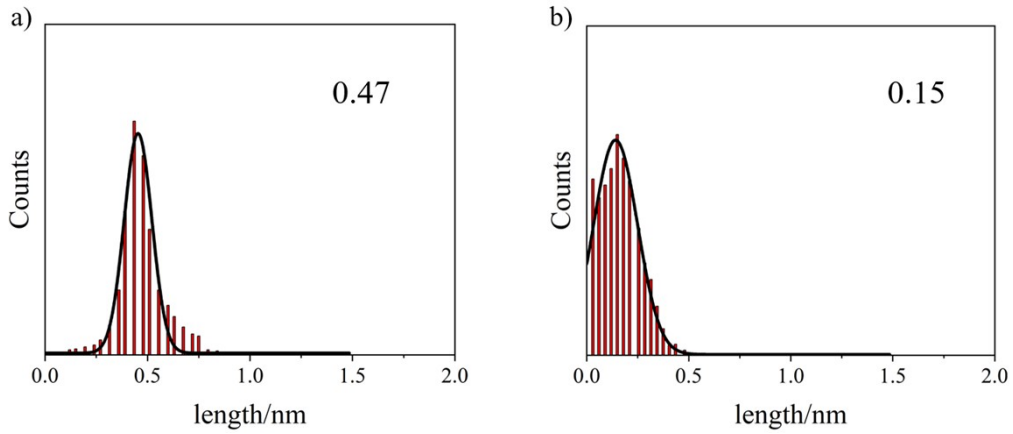

Figure S8. Displacement distribution histograms of single molecular junctions with molecules. (a) **p=p**, (b) **m=m**

DFT calcualtions

The geometry optimizations of the molecules were carried out using ωB97XD functional and 6-311G(d,p) basis set in Gaussian 09 package, and the frequency analysis was performed at the same theoretical level to verify that the stationary points are minimums or transition states. Then, the optimized molecular structures were placed between two gold electrodes to construct the single-molecule junctions. The surface configuration of the gold electrode was constructed as a pyramid. In the initial configuration of the device, the distance between the N atom and the gold atom of the electrode was controlled at about 2.3 Å. In configuration optimization, the coordinates of all gold atoms in the electrode were fixed and there were no restrictions on the coordinates of the molecules. The geometry optimization and the transmission spectrum of single-molecule junction were performed using the Quantum ATKQ-2021.06 package. The FHI pseudopotential with a double-ζ basis set was used for Au atoms, and the PseudoDojo pseudopotential with a medium basis set was used for other atoms. A real-space grid with an equivalent energy cutoff of 80 Hartree and the k-points of 3, 3, 134 was used for geometry optimization, and the force threshold is 0.05 eV/Å. In the transmission calculation, transverse k points are increased to 7, 7. The Au−N is about 2.2 Å and coplanar with the thiazole ring in the initial configurations of the molecular junctions.

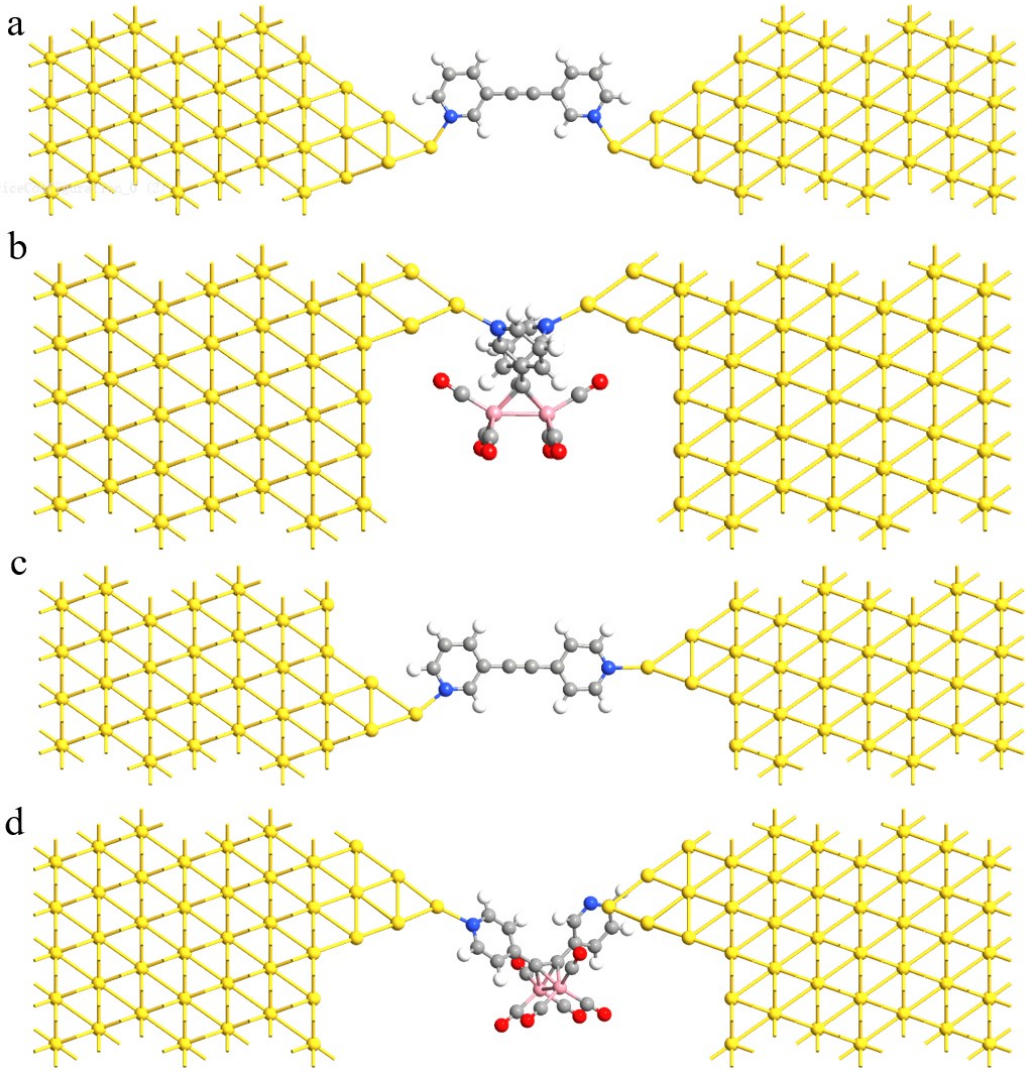

Figure S9. The idealized device configuration of (a) **m-m**, (b) **m-Co-m**, (c) **p-m** and (d) **p-Co-m**.

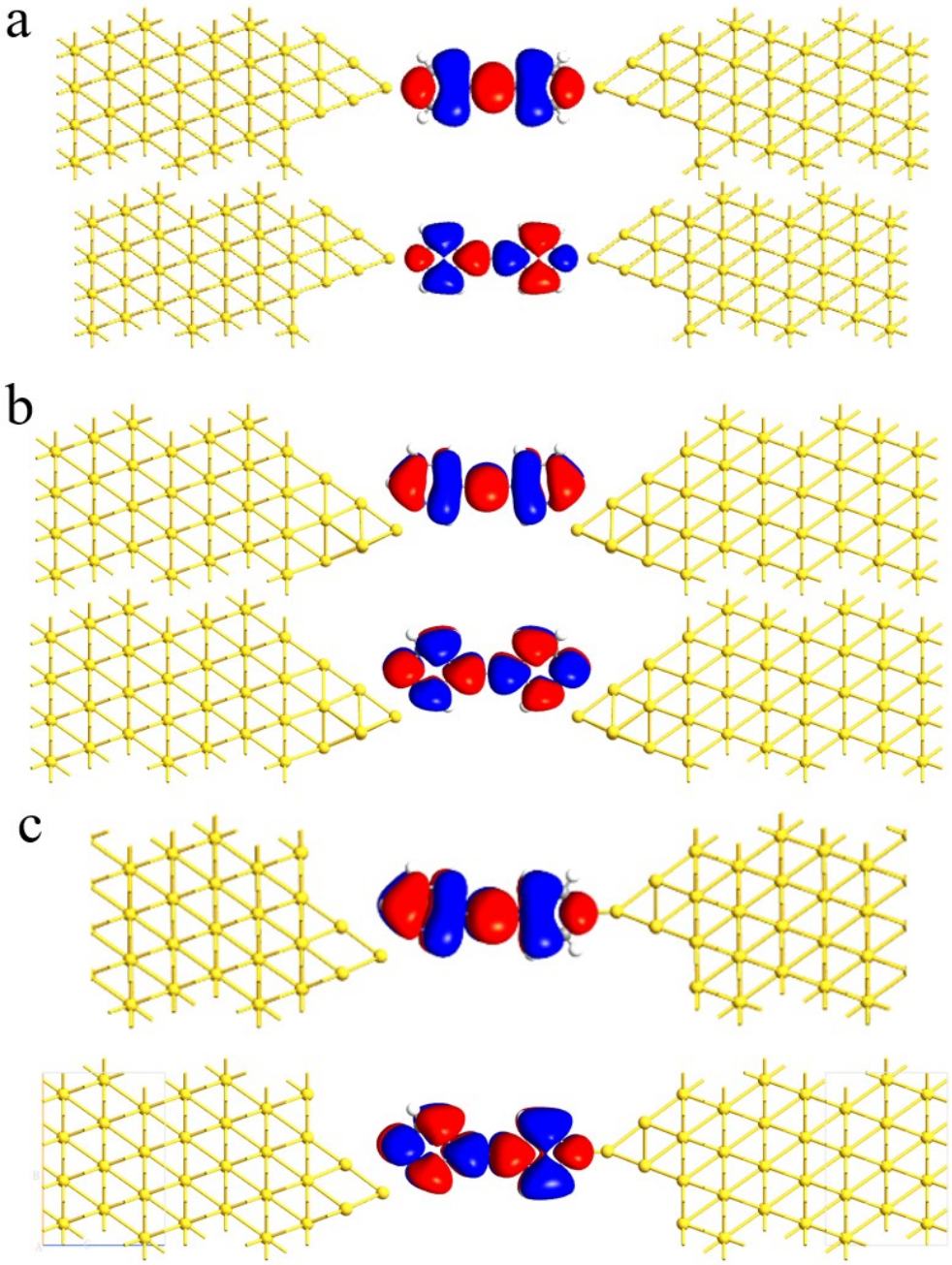

Figure S10. The MPSH plots for (a) **p-p** (b) **m-m** and (c) **p-m**. The upper is the HOMO orbital and the lower is the LUMO orbital.

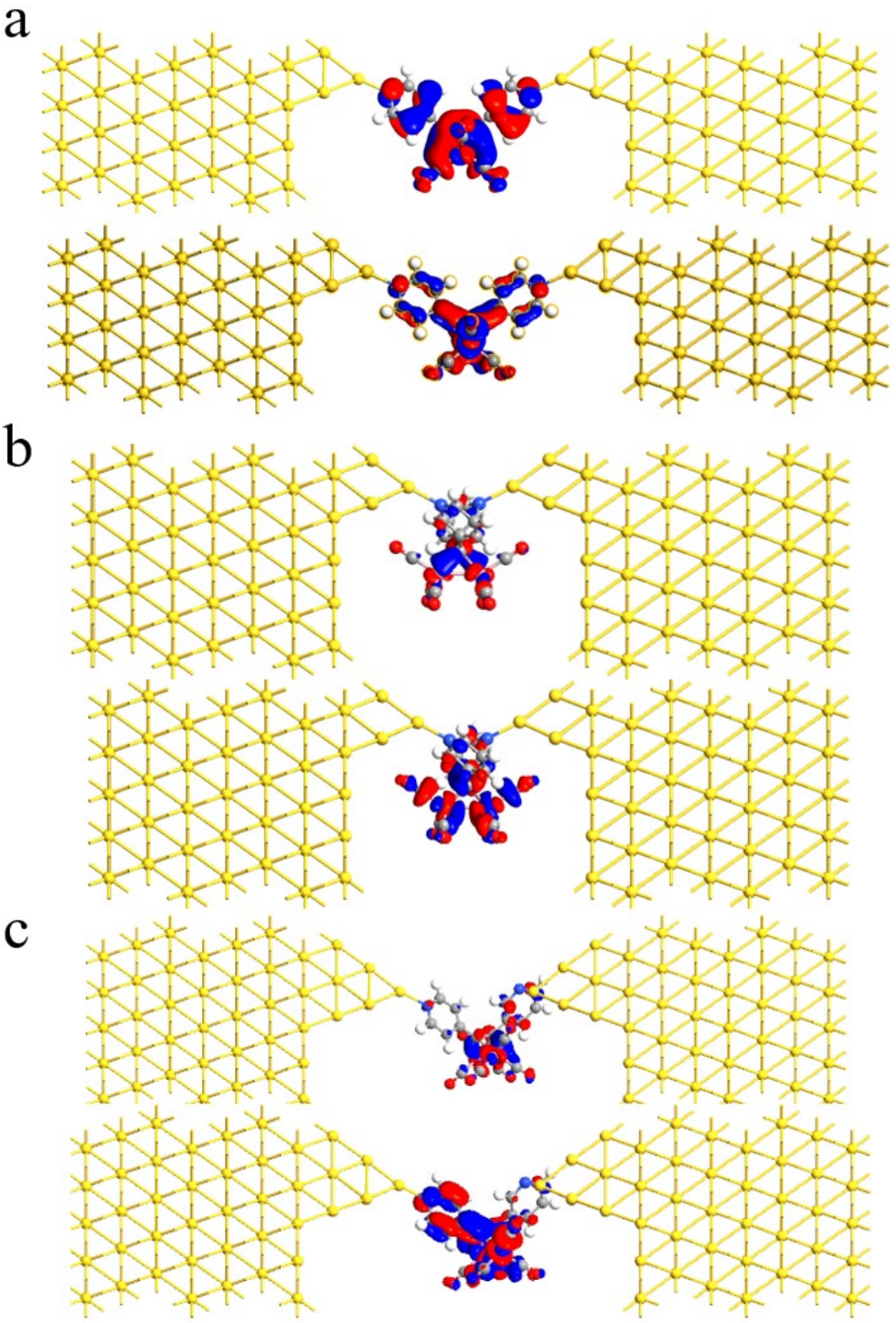

Figure S11. The MPSH plots for (a) **p-Co-p** (b) **m-Co-m** and (c) **p-Co-m**. The upper is the HOMO orbital and the lower is the LUMO orbital.

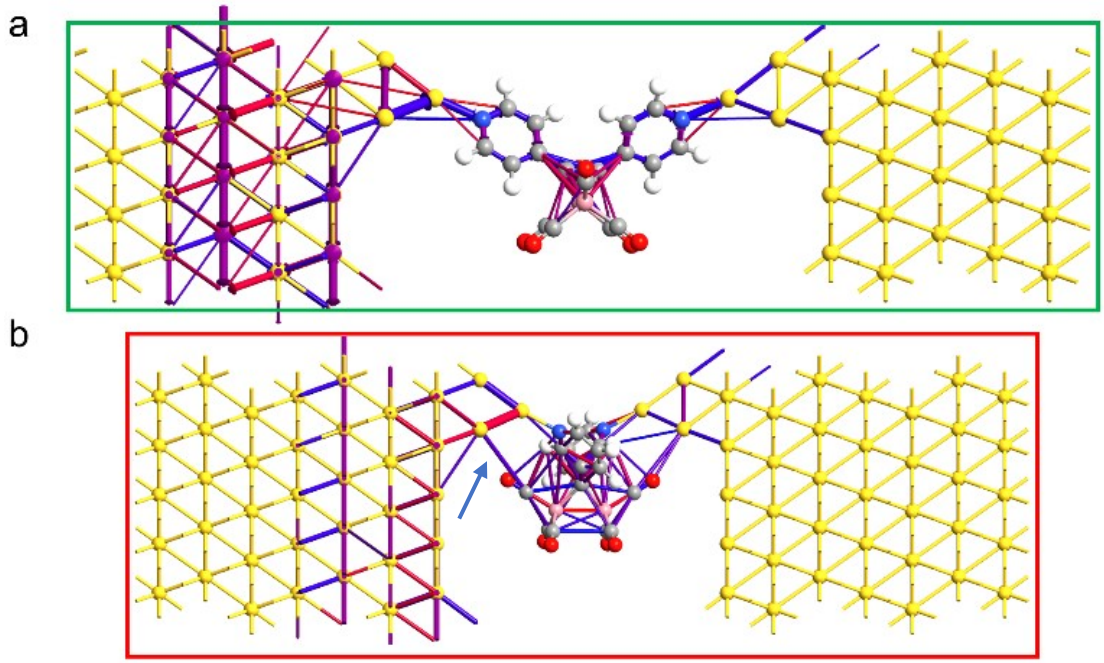

Figure S12. The transmission pathways of (a) **p-Co-p** (b) **m-Co-m.**

	HOMO (eV)	LUMO (eV)	gap (eV)
p-p	-6.67	-2.12	4.55
p-m	-6.43	-1.94	4.49
m-m	-6.20	-1.76	4.44
p-Co-p	-6.57	-2.83	3.74
p-Co-m	-6.44	-2.75	3.69
m-Co-m	-6.32	-2.67	3.65

Table S1. The energy level of molecules involved

Reference

1. Harry L, Anderson; Christopher J, Walter; Anton, V.-F.; Robert A, Hay; Philip A, Lowden; Jeremy K, M. S. *J. Chem. Soc. Perkin Trans. 1* **1995,** *24,*3537-3733.

2. Sergey, P. G.; Artem, I. V.; Evgeny, N. U.; Natalia, A. L.; Asya, A. B.; Lyudmila, G. K.; Andrei, V. C.; Yuri, A. S.; Michael, V. A.; Judith, A. K. H.; Dan, J.; Ulf, G. E. *New J. Chem*. **2005**, *29*, 881–894.

3. Song, L.-C.; Jin, G.-X.; Wang, H.-T.; Zhang, W.-X.; Hu, Q.-M. *Organometallics* **2005**, *24*, 6464-6471.

4. Liu, D.; Zhang, Y.; Zhan, L.; Lau, T.-K.; Yin, H.; Fong, P. W. K.; So, S.; Zhang, S.; Lu, X.; Hou, J.; Chen, H.; Wong, W.; Li, G. *J. Mater. Chem. A.* **2019**, *7*, 14153.

5. Arroyo, C. R.; Tarkuc, Simge.; Frisenda, R.; Seldenthuis, J. S.; Woerde, C. H. M.; Eelkema, Rienk.; Grozema, F. C.; van der Zant, H. S. J. *Angew. Chem. Int. Ed.* **2013**, *52*, 3152.

6. Liu, J.; Zhao, X.; Zheng, J.; Huang, X.; Tang, Y.; Wang, F.; Li, R.; Pi, J.; Huang, C.; Wang, L.; Yang, Y.; Shi, J.; Mao, B.-W.; Tian, Z.-Q.; Bryce, M. R.; Hong, W. *Chem* **2019**, *5*, 390.

7. Bai, J.; Daaoub, A.; Sangtarash, S.; Li, X.;Tang, Y.; Zou, Q.; Sadeghi, H.; Liu, S.; Huang, X.; Tan, Z.; Liu, J.; Yang, Y.; Shi, J.; Mészáros, G.; Chen, W.; Lambert, C.; Hong, W. *Nat. Mater.* **2019**, *18*, 364.

8. Tang, C.; Chen, L.; Zhang, L.; Chen, Z.; Li, G.; Yan, Z.; Lin, L.; Liu, J.; Huang, L.; Ye, Y.; Hua, Y.; Shi, J.; Xia, H.; Hong, W. *Angew. Chem. Int. Ed.* **2019**, *58*, 10601.